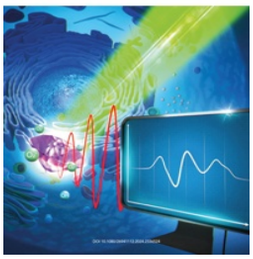
FUNCTIONAL DIAMOND



Functional Diamond

ISSN: 2694-1112 (Print) 2694-1120 (Online) Journal homepage: www.tandfonline.com/journals/tfdi20

First-principles study of nitrogen-mediated Be doping for p-type diamond

Cong Li, Shaoheng Cheng, Nan Gao & Hongdong Li

To cite this article: Cong Li, Shaoheng Cheng, Nan Gao & Hongdong Li (2026) First-principles study of nitrogen-mediated Be doping for p-type diamond, Functional Diamond, 6:1, 2601403, DOI: 10.1080/26941112.2025.2601403

To link to this article: https://doi.org/10.1080/26941112.2025.2601403

© 2026 The Author(s). Published by Informa UK Limited, trading as Taylor & Francis Group, on behalf of Zhengzhou Research Institute for Abrasives & Grinding Co., Ltd.

View supplementary material

Published online: 05 Jan 2026.

Submit your article to this journal

Article views: 243

View related articles

View Crossmark data

Full Terms & Conditions of access and use can be found at
https://www.tandfonline.com/action/journalInformation?journalCode=tfdi20

FUNCTIONAL DIAMOND
2026, VOL. 6, NO. 1, 2601403
https://doi.org/10.1080/26941112.2025.2601403

Taylor & Francis
Taylor & Francis Group

RESEARCH ARTICLE

OPEN ACCESS Check for updates

First-principles study of nitrogen-mediated Be doping for p-type diamond

Cong Li, Shaoheng Cheng, Nan Gao, and Hongdong Li

State Key Lab of High Pressure and Superhard Materials, College of Physics, Jilin University, Changchun, China

ABSTRACT

Achieving efficient p-type conductivity is essential for advancing diamond-based high-power and high-frequency electronic devices. In this study, we employ first-principles calculation to evaluate Be as a p-type dopant in diamond and investigate the synergistic enhancement achieved through N-Be co-doping. The high-concentration Be doping can significantly reduce the acceptor ionization energy to 0.35 eV. More importantly, N-Be co-doping substantially reduces defect formation energies and acceptor ionization energies, N-4Be co-doped structure shows the reduced formation energy of 3.37 eV and acceptor ionization energy as low as 0.30 eV. These findings pave the way for the experimental realization of high-performance diamond-based electronic devices and suggest the potential for exploring donor–acceptor co-doping to achieve efficient p-type conductivity.

ARTICLE HISTORY
Received 30 October 2025
Accepted 4 December 2025

KEYWORDS
Acceptor ionization energy; diamond; formation energy; p-type doping

1. Introduction

Diamond, as an ultrawide-bandgap semiconductor, exhibits exceptional physical and chemical properties, making it a promising candidate for high-frequency, high-power, irradiation-tolerant, and high-temperature electronic applications [1,2]. To facilitate its widespread integration into electronic devices, significant efforts have been devoted to engineering diamond with superior n-type and p-type conductivity through doping with donor and acceptor impurities [3–5]. Phosphorus (P)-doped diamond, the most prevalent type of n-type diamond, is still limited by the low solubility of P dopant [6] and undesirable compensating defects [7,8]. In order to overcome this limitation, strain engineering has been suggested as a promising avenue to reduce the formation energy and ionization energy, as well as suppress compensating defects [9]. Boron (B) doping has been widely used as an effective approach to induce p-type conductivity in diamond [10–12], whose activation energy is about 0.36 eV, and the doping range is relatively wide (10^{14} and 10^{21} cm^{-3}) [13]. The high carrier concentration (1.8×10^{21} cm^{-3}) [14] and carrier mobility (1550–2200 $cm^2V^{-1}s^{-1}$) [15] have been reported for B-doped diamond. However, its electronic application is limited by the deep acceptor levels, which only activate low carriers at room temperature and fail to meet the requirements of practical semiconductor device applications [16]. Thus, it is necessary to explore alternative p-type dopants with a shallower acceptor level.

Beryllium (Be) is a neighboring element to B, with two electrons in its outer electronic shell, thus, its substitution is expected to be an acceptor. Be atom has been extensively employed as a p-type dopant in wide-bandgap semiconductors GaAs and GaN [17–19], while also being employed to modify the properties of graphene, fullerenes, and carbon nanotubes [20]. It motivates the investigation of Be doping in diamond. Ueda et al. achieved controlled Be concentration doping in diamond by inserting a solid Be-rod into the plasma ball during microwave plasma chemical vapor deposition (CVD) growth [21]. Although introducing Be atoms in diamond at interstitial sites can form shallow level [22], its formation energy (8.03 eV) is much higher than that of substitution defect (2.85 eV) [23]. The substitutional defect of Be in diamond shows high activation energy (1.22 eV), which prevents sufficient carrier generation at room temperature [23]. Thus, both the formation energy and ionization energy for Be-doped diamond should be reduced. Previous theoretical studies had revealed that increasing the B impurity concentration enhanced its solubility in diamond [24] and significantly reduced the ionization energy, favoring the formation of double-acceptor p-type diamond [25]. Furthermore, experimental results indicated that a linear increase in charge transfer resistance was highly dependent on B concentration, and optimal electrochemical performance near the phase separation limit was attributed to a higher effective doping [18]. Thus, it is supposed that

CONTACT Nan Gao gaon@jlu.edu.cn; Hongdong Li hdli@jlu.edu.cn
Supplemental data for this article can be accessed online at https://doi.org/10.1080/26941112.2025.2601403.
© 2026 The Author(s). Published by Informa UK Limited, trading as Taylor & Francis Group, on behalf of Zhengzhou Research Institute for Abrasives & Grinding Co., Ltd.
This is an Open Access article distributed under the terms of the Creative Commons Attribution-NonCommercial License (http://creativecommons.org/licenses/by-nc/4.0/), which permits unrestricted non-commercial use, distribution, and reproduction in any medium, provided the original work is properly cited. The terms on which this article has been published allow the posting of the Accepted Manuscript in a repository by the author(s) or with their consent.

increasing the dopant concentration could decrease the activation energy of Be-doped diamond. However, the practical viability of Be doping, including the solubility and stability of Be-related defect complexes, remains insufficiently explored.

Based on these considerations, in this work, we systematically investigate the structural stability, electronic structure, defect formation energy, and acceptor ionization energy for Be and Be-nitrogen (N) co-doped diamond using first-principles calculation. Our work clarifies the feasibility and advantages of Be as an alternative to B, and reveals the synergistic role of N in reducing formation energies and acceptor ionization energies. These findings establish a theoretical foundation for understanding the fundamental physics of p-type doping in diamond and offer practical design guidelines for developing efficient and stable diamond-based electronic devices.

2. Calculation methods

The geometry optimization and property calculations were performed by the density functional theory (DFT) [26] combined with the projector augmented wave (PAW) potentials [27], which were implemented in the Vienna ab initio Simulation Package (VASP) [28]. The Perdew–Burke–Ernzerhof (PBE) functional within the generalized gradient approximation (GGA) was employed as the exchange–correlation functional [29]. Spin-polarized calculations were performed for all systems. In this work, a plane-wave cutoff energy of 520 eV was employed, with a $3\times3\times3$ k-point mesh for Brillouin zone integration. The energy convergence criterion was set to 1×10^{-5} eV, and the force convergence criterion was 0.001 eV/Å. After the supercell size test (Table S1), the $3\times3\times3$ supercell of diamond containing 216 atoms was used in this work for reasonable accuracy and higher efficiency.

To evaluate the structural stability and doping efficiency, the formation energy (E_f) of the impurity X in neutral charge state ($q=0$) is defined as [30]:

$$E_f\left[X^0\right]=E_{tot}\left[X,0\right]-E_{tot}\left[C,bulk\right]-\sum\nolimits_x n_x\mu_x \quad (1)$$

where $E_{\rm tot}$ [X, 0] and $E_{\rm tot}$ [C, $bulk$] are the total energies of diamond supercell those include the impurity X and the prefect diamond, respectively. n_x describes the number of adding impurity atoms or removing C atoms, and μ_x is the corresponding chemical potential of impurity X. The chemical potentials of C, B, N and Be are calculated from bulk diamond, B_2H_6, N_2 and bulk Be, respectively.

For calculating the ionization energy, we focus on the formation energy of impurity X with charge state q, which is defined as [30]:

$$E_f\left[X^q\right]=E_{tot}\left[X,q\right]-E_{tot}\left[C,bulk\right]-\sum\nolimits_x n_x\mu_x+q\left(E_F+E_{VBM}+\Delta V\right)+E_{corr} \quad (2)$$

where E_{tot} [X,q] is the total energy of diamond containing impurities X in charge state q. E_F is the Fermi level referenced to the valence band maximum (VBM) of perfect diamond, and ΔV is a correction for aligning the electrostatic potentials between the prefect and the defect supercells. The image charge interaction term $E_{\rm corr}$ is [31,32]:

$$E_{corr}=\left(1+f\right)\frac{q^2\alpha}{2\varepsilon L} \quad (3)$$

where f is −0.34 for the diamond lattice, α is the lattice-dependent Madelung constant [33], ε is the dielectric constant (5.5 for diamond) [34], and L is the lattice constant.

3. Results and discussion

3.1. Be-doped diamond structure

As shown in Figure 1, Be-doped diamond structures are constructed by substituting two to five carbon atoms with Be atoms. These configurations are designated as 2Be, 3Be, 4Be, and 5Be. Only adjacent substitution sites are considered, since they exhibit lower formation energies than separated substitution sites (Table S2). The Be–C bond lengths are slightly larger than the B–C bond lengths in analogous B-doped structures (Figure S1), which is attributed to the larger atomic radius of Be compared to that of B.

The band structures for the 2Be, 3Be, 4Be, and 5Be configurations are shown in Figure 2. For all structures, an impurity band is observed near the Fermi level, with an additional band emerging just below the conduction band minimum (CBM). It suggests that the p-type character is preserved with increasing Be doping concentration. For the 2Be system (Figure 2a), spin splitting is observed, indicating the existence of spin-polarized electronic states arising from the asymmetric distribution of electron spins due to Be doping. In contrast, the 3Be, 4Be, and 5Be systems (Figures 2b–d) do not show spin splitting, since the spin-up bands coincide with the spin-down bands, suggesting that spin polarization is restored at higher Be concentrations.

The corresponding projected density of states (PDOS) in Figure 3 show that the impurity band primarily originates from the p-orbitals of both C and Be atoms and exhibits a clear dependence on doping concentration. In the 2Be system (Figure 3a), the absence of significant contribution from Be to the CBM. For the 3Be system in Figure 3b, the impurity states near the CBM originate from both the s- and p-orbitals of C and Be atoms, while

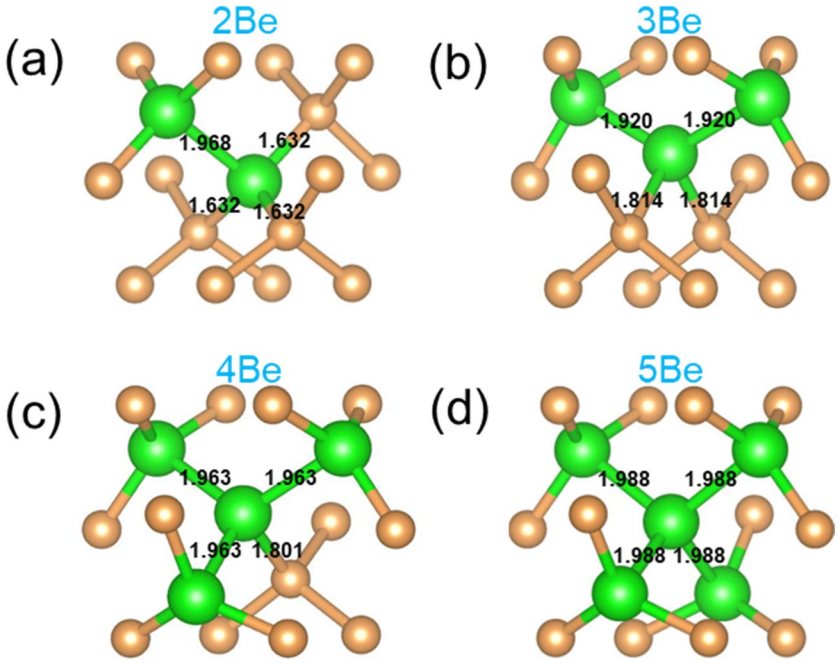


Figure 1. Structural models of Be-doped diamond for (a) 2Be, (b) 3Be, (c) 4Be, (d) 5Be structures. The yellow and green balls represent C and Be atoms. The bond lengths near the dopants are labeled.

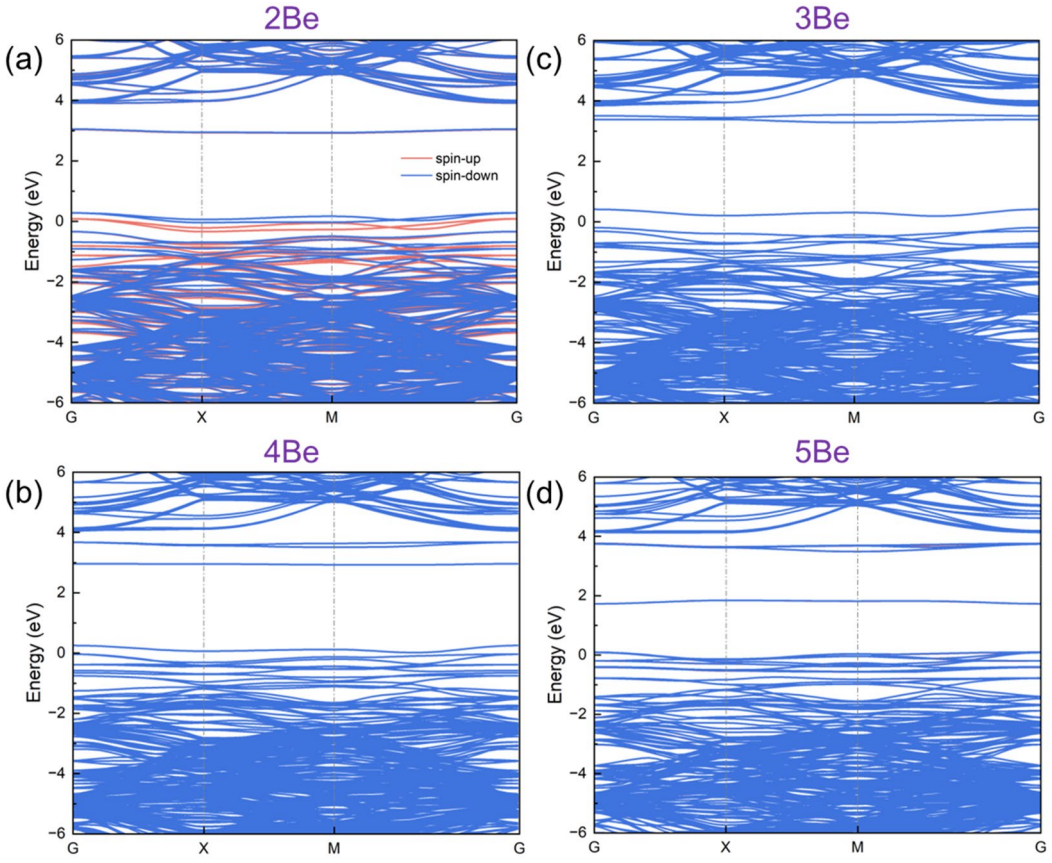


Figure 2. Spin-polarized band structures of (a) 2Be, (b) 3Be, (c) 4Be and (d) 5Be doping in diamond. The Fermi level is set at zero.

the impurity states near the VBM contribute solely from the p-orbitals. As the Be concentration increases to 4Be (Figure 3c) and 5Be (Figure 3d), the contributions from the s- and p-orbitals of Be rise significantly. The Be contribution of p-orbitals from the impurity level near the CBM becomes increasingly dominant, indicating strong orbital hybridization between Be and C atoms.

The ionization energy is a critical parameter for doped materials. The thermodynamic transition level $\varepsilon(q_1/q_2)$ is used to estimate the ionization energy. It is

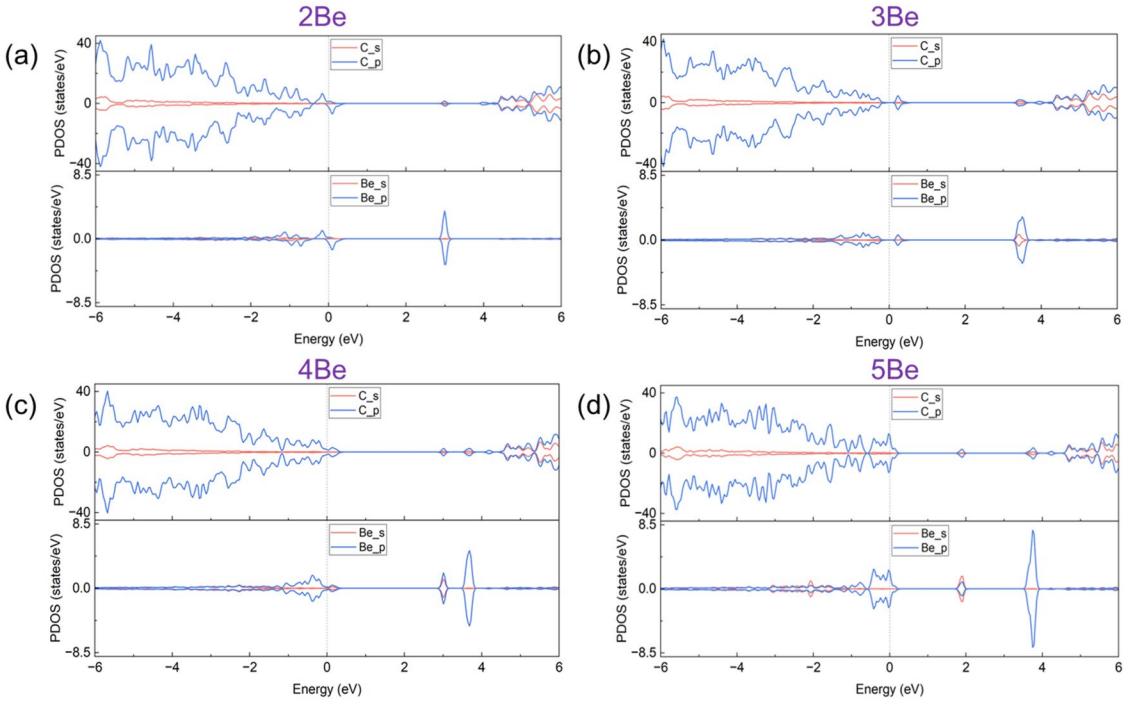


Figure 3. Partial density of states (PDOS) of (a) 2Be, (b) 3Be, (c) 4Be and (d) 5Be doping in diamond. The Fermi level is set at zero.

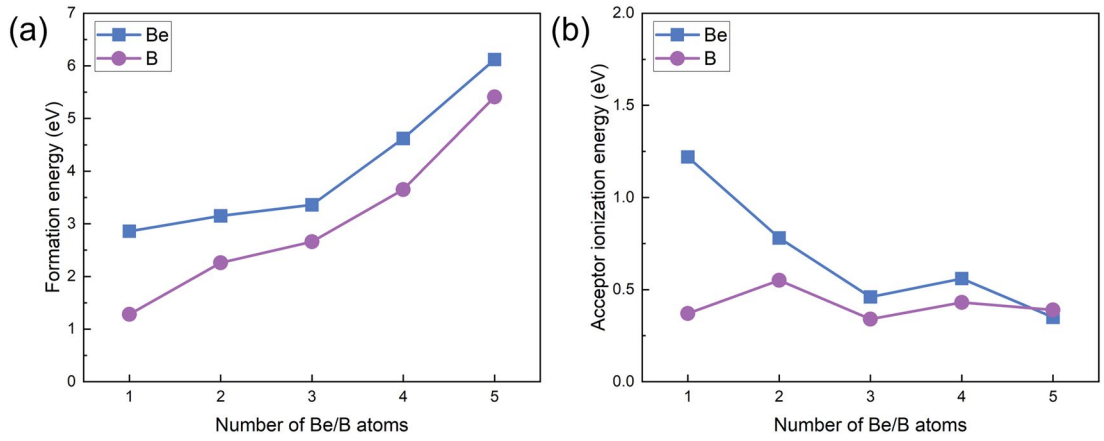


Figure 4. (a) Formation energies (E_f) and (b) acceptor ionization energies (E_a) for Be and B doping in diamond as a function of dopant atom concentration.

defined as the Fermi level position at which the formation energies of charge states q_1 and q_2 are equal [35]:

$$\varepsilon(q_1/q_2) = \frac{E_f\left[X^{q_1};E_F=0\right]-E_f\left[X^{q_2};E_F=0\right]}{q_2-q_1} - (E_v+\Delta V) \tag{4}$$

where $E_f\left[X^{q_1};E_F=0\right]$ and $E_f\left[X^{q_2};E_F=0\right]$ are the formation energies of the supercell containing the impurity in charge states q_1 and q_2, respectively. The acceptor level (−1/0) corresponds to the ionization energy E_a for acceptor [35,36].

As summarized in Figure 4, the acceptor ionization energies for single Be and B dopants are 1.22 eV and 0.37 eV, respectively, in excellent agreement with previous values (1.18 eV [37] and 0.38 eV [25]). As the concentration of the Be dopant increases, the formation energies for the 2Be, 3Be, 4Be, and 5Be configurations rise to 3.15 eV, 3.36 eV, 4.62 eV, and 6.12 eV, respectively. It is attributed to the enhanced lattice distortion induced by the incorporation of multiple dopant atoms. In addition, the formation energy is only slightly larger than that of B-doped diamond. Correspondingly, the acceptor energies for Be-doped diamond decrease to 0.78 eV, 0.46 eV, 0.56 eV, and 0.35 eV, indicating improved carrier activation efficiency at higher doping levels. The values are comparable with those for B-doped diamond (0.90 eV, 0.34 eV, 0.78 eV, and 0.39 eV). Consequently, Be doping is less effective than B doping for achieving p-type conductivity in diamond, since the former generally

exhibits higher formation energies and comparable or higher acceptor ionization energies across the investigated configurations.

3.2. N-Be co-doped diamond structures

Co-doping strategies, which involve the introduction of an additional element alongside the primary dopant, could enhance dopant solubility and modify electronic properties [25]. N, as a donor, introduces excess electrons those can partially compensate for the holes generated by acceptors. The introducing N atom has been found to mitigate lattice strain and passivate detrimental defects, leading to reduced defect formation energies and ionization energies [37–40]. The smaller covalent radius of N relative to C would help to mitigate lattice distortion induced by the larger Be atoms.

In the N–1Be co-doped configuration (Figure 5a), the N–Be and N–C bond lengths are 1.618 Å and 1.515 Å, respectively. The N-2Be complex (Figure 5b) has two N–Be bonds of 1.587 Å and two N–C bonds of 1.469 Å. The N-3Be configuration in Figure 5c exhibits one N–C bond length of 1.395 Å and three N–Be bond lengths of 1.571 Å. In the N-4Be case (Figure 5d), the N atom occupies the central tetrahedral site, forming four equivalent N–Be bonds of 1.525 Å. Similarly, N–B co-doped structures are shown in Figure S2. In the N–B complex, the N–C bond length is longer than that in the analogous N–Be structure.

As shown in Figure 6, the band structures of N–Be co-doped system retains p-type conductivity, as evidenced by the position of the Fermi level within the VBM. Notably, N-Be co-doped systems all exhibit spin asymmetry near the Fermi level, indicating the persistence of spin-polarized electronic states across different Be concentrations. The presence of N atoms thus plays a crucial role in stabilizing spin polarization, as Be concentration increases.

For the PDOS of N–1Be (Figure 7a), the impurity states within the VBM are dominated by p-orbitals of C and Be. N contributions become evident in the N–2Be case (Figure 7b), indicating that N atoms actively participate in orbital interactions with both C and Be atoms. In the N–3Be and N–4Be complexes (Figures 7c and d), the impurity states shift to higher energies above the VBM and exhibit hybridized contributions from the p-orbitals of C, Be, and N. In contrast, the VBM is dominated by C and Be states. The band structures and PDOS for N–B co-doped diamond are shown in Figure S3. Except for N-1B exhibiting insulating properties, N-2B, N-3B, and N-4B display p-type characteristics with no impurity levels. It is well known that the PBE functional underestimates the bandgap, and hybrid functionals provide a more accurate description of the bandgap [41]. However, for computational efficiency, we only perform additional PDOS calculations using the Heyd–Scuseria–Ernzerhof functional (HSE06) [42] for the 5Be and N-4Be configurations. The results in Figure S4 show the similar features, and their fundamental electronic characteristics and p-type nature are consistent with the PBE results.

The formation energy and acceptor ionization energy are summarized in Figure 8. For the N–Be

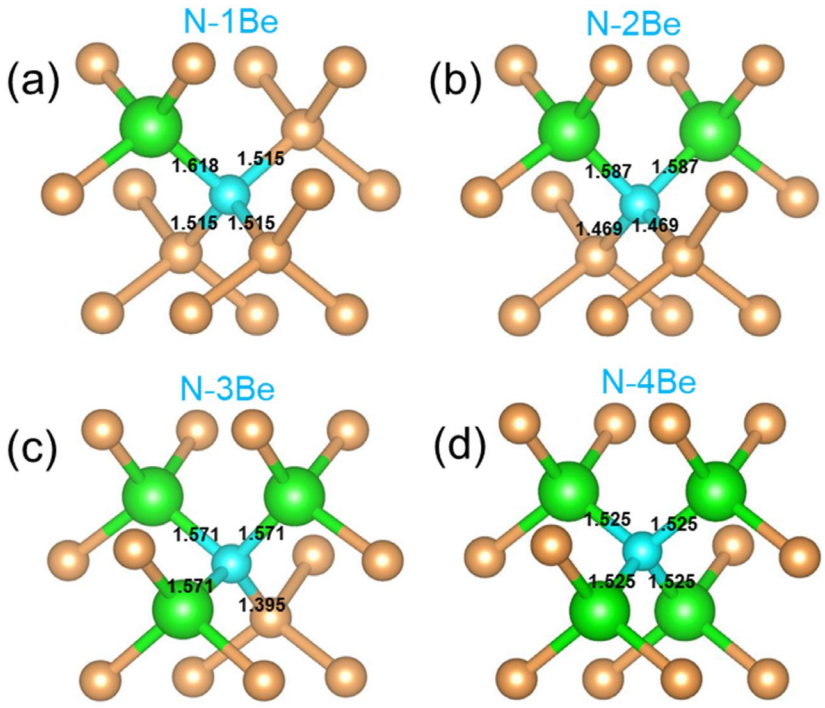


Figure 5. Structural models of N-Be co-doped diamond for (a) N-1Be, (b) N-2Be, (c) N-3Be, (d) N-4Be structures. The yellow, green and blue balls represent C, Be and N atoms, respectively. The bond lengths near the dopants are labeled.

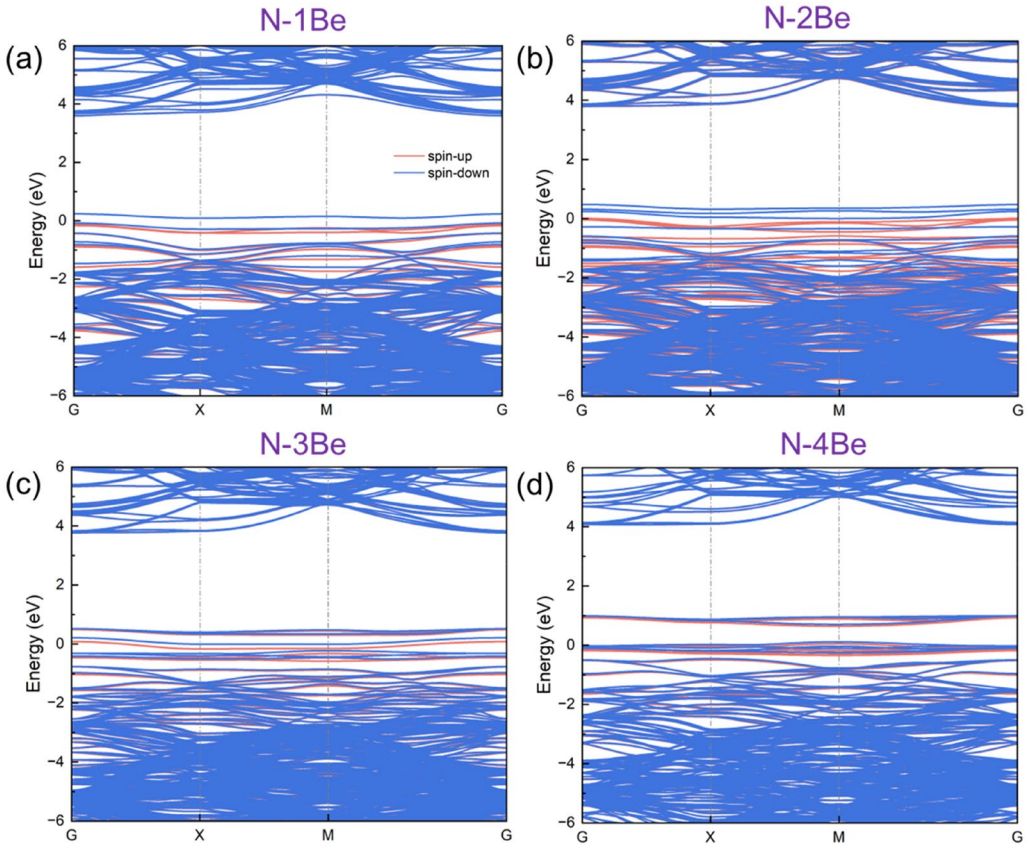


Figure 6. Spin-polarized band structures of (a) N-1Be, (b) N-2Be, (c) N-3Be and (d) N-4Be doping in diamond, respectively. The Fermi level is set at zero.

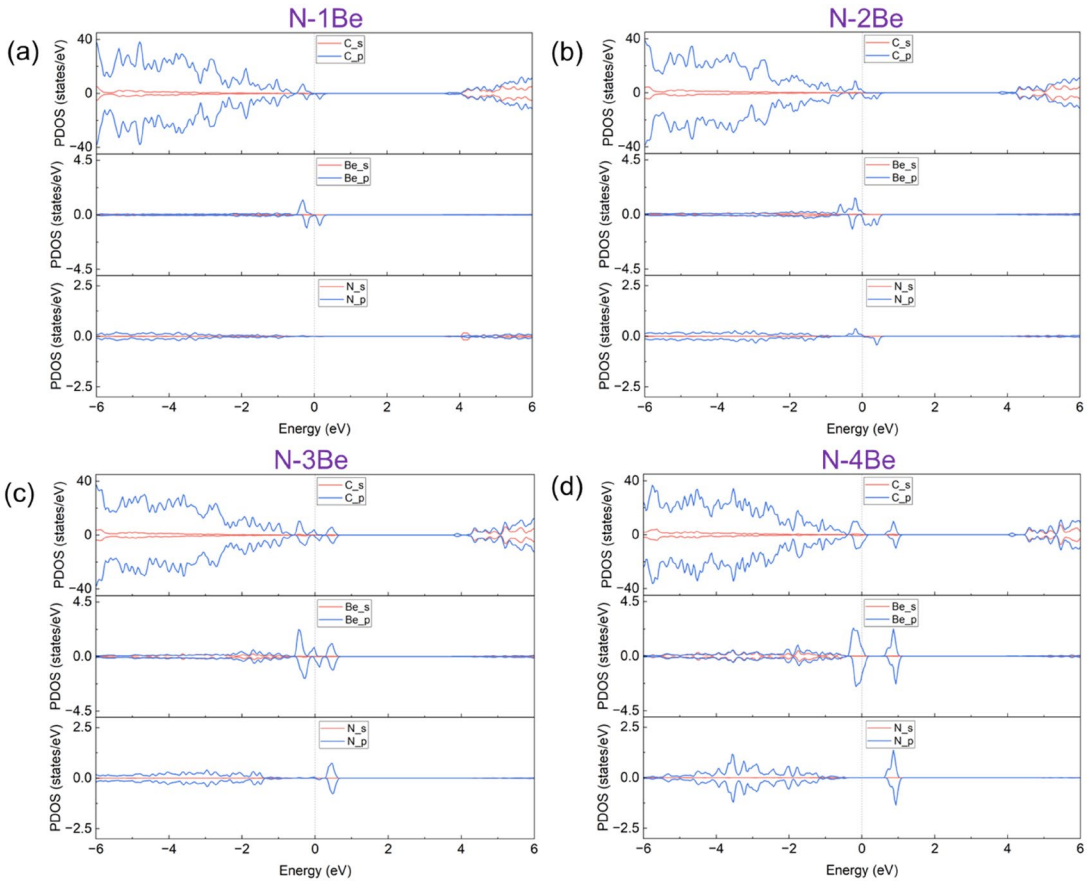


Figure 7. Partial density of states (PDOS) of (a) N-1Be, (b) N-2Be, (c) N-3Be and (d) N-4Be doping in diamond, respectively. The Fermi level is set at zero.

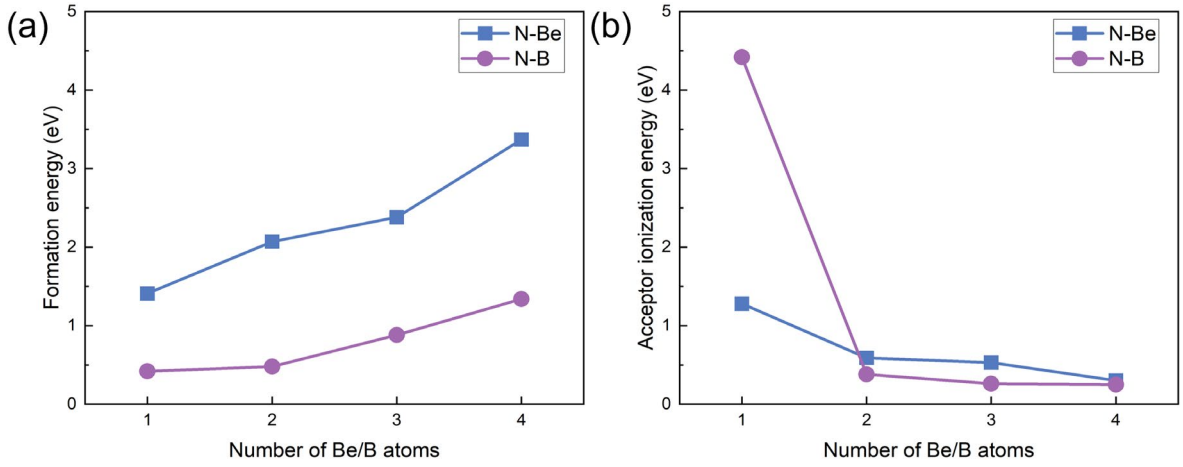


Figure 8. (a) Formation energies (E_f) and (b) acceptor ionization energies (E_a) for N-Be and N-B co-doped diamond as a function of dopant atom concentration.

co-doped systems, the formation energies are 1.41 eV, 2.07 eV, 2.38 eV, and 3.37 eV, which are significantly smaller than those for single Be-doped diamond in Figure 4. In contrast, N–B co-doped configurations exhibit lower formation energies of 0.42 eV, 0.48 eV, 0.88 eV, and 1.34 eV, highlighting their superior dopant solubility. As discussed previously, the N–1B complex exhibits insulating behavior, the thermodynamic transition level between the (0/+1) charge states is located near the VBM, resulting in a very large acceptor ionization energy of 4.42 eV, which is consistent with the reported value of 4.41 eV [43]. The acceptor ionization energies for N-2B, N-3B, and N-4B are 0.38 eV, 0.26 eV, and 0.25 eV, and the corresponding values of 1.28 eV, 0.59 eV, 0.53 eV, and 0.30 eV for N-1Be, N-2Be, N-3Be, N-4Be structures, respectively, approaching the shallow-acceptor limit in diamond. Thus, the configurations with a N atom bonded to adjacent Be or B atoms exhibit markedly lower formation energy and acceptor ionization energy compared to their single-doped counterparts, confirming that N-mediated co-doping significantly stabilizes impurity incorporation.

To elucidate the underlying mechanism of N reducing the formation energy and acceptor ionization energy of the Be acceptor, we perform quantitative analyses of the N-4Be co-doped structure. Figure S5a shows the remarkable charge redistribution near the dopants, there is the electron accumulation around the N atom and the electron depletion around the Be atom, being consistent with the Bader charge analysis (the central N gains +1.94 *e*, and each Be loses −1.55 *e*). The Crystal Orbital Hamiltonian Population (COHP) analysis for the N-Be bond in the N-4Be configuration provides quantitative measure of the bond strength. As shown in Figure S5b, the N-Be bonding states are predominantly located below the Fermi level, and the integrated ICOHP value is calculated to be −1.101 eV. This value is more negative than that of the Be-C bond (−0.822 eV) in Figure S5c, indicating a stronger covalent interaction between N and Be. This enhanced bonding contributes substantially to the structural stabilization and the reduction of E_f and E_a.

4. Conclusion

In summary, this study systematically investigates the structural models and p-type doping performance of Be-doped and N–Be co-doped diamond using first-principles calculation. Our results demonstrate that Be dopants can induce p-type conductivity in diamond, and high-concentration Be doping reduces the acceptor ionization energy to 0.35 eV, which is beneficial for enhancing carrier activation efficiency. Furthermore, N-Be co-doping structures exhibit substantially reduced formation energies and lower ionization energies compared to single Be doping, with formation energy of 3.37 eV and acceptor ionization energy as low as 0.30 eV for the N-4Be configuration. These findings suggest the potential for exploring other donor–acceptor co-doping combinations to achieve efficient p-type conductivity.

Disclosure of interest

The authors report there are no competing interests to declare.

This work was supported by the Key Science and Technology Special Project of Jilin Province (No. 20240211001GX). Computation was carried out at the High-Performance Computing Center of Jilin University. The authors acknowledge the Jilin University Lixin Excellent Young Teacher Training Program.

Funding

This work was supported by the Key Science and Technology Special Project of Jilin Province (No. 20240211001GX). Computation was carried out at the High-Performance Computing Center of Jilin University. The authors acknowledge the Jilin University Lixin Excellent Young Teacher Training Program.

Notes on contributors

Cong Li, M.S. candidate at State Key Lab of High Pressure and Superhard Materials, College of Physics, Jilin University, Jilin, China. Her research focuses on the theoretical design of semiconductor doping in diamond.

Nan Gao, Professor, working at State Key Lab of High Pressure and Superhard Materials, College of Physics, Jilin University, Jilin, China. Her research focuses on theoretical calculations, and eletrochemical applications of functional diamond.

Shaoheng Cheng, Professor, working at State Key Lab of High Pressure and Superhard Materials, College of Physics, Jilin University, Jilin, China. His research focuses on preparation, characterization, device applications of CVD diamonds.

Hongdong Li, Professor and Group Leader, working in State Key Lab of High Pressure and Superhard Materials, College of Physics, Jilin University, Jilin, China. His research interests include the preparation, characterization, devices, theoretical calculations, and applications of multifunctional diamond polycrystalline films, single crystal diamons, and various diamond nano-structures.

ORCID

Nan Gao http://orcid.org/0000-0003-2374-3205
Hongdong Li http://orcid.org/0000-0002-5555-935X

References

[1] Wort CJH, Balmer RS. Diamond as an electronic material. Mater Tod. 2008;11(1–2):22–28. doi: 10.1016/S1369-7021(07)70349-8
[2] Koizumi S, Watanabe K, Hasegawa M, et al. Ultraviolet emission from a diamond pn junction. Science (1979). 2001;292(5523):1899–1901. doi: 10.1126/science.1060258
[3] Nesladek M. Conventional n-type doping in diamond: state of the art and recent progress. Semicond Sci Technol. 2005;20(2):R19–R27. doi: 10.1088/0268-1242/20/2/R01
[4] Traoré A, Koizumi S, Pernot J. Effect of n- and p-type doping concentrations and compensation on the electrical properties of semiconducting diamond. Phys Status Solidi A. 2016;213(8):2036–2043. doi: 10.1002/pssa.201600407
[5] Pinault M-A, Barjon J, Kociniewski T, et al. The n-type doping of diamond: present status and pending questions. Phys B Condens Matter. 2007;401–402:51–56. doi: 10.1016/j.physb.2007.08.112
[6] Yan CX, Dai Y, Guo M, et al. Theoretical characterization of carrier compensation in P-doped diamond. Appl Surf Sci. 2009;255(7):3994–4000. doi: 10.1016/j.apsusc.2008.10.092
[7] Miyazaki T, Yamasaki S. Ab initio energetics of phosphorus related complex defects in synthetic diamond. Phys B Condens Matter. 2006;376–377:304–306. doi: 10.1016/j.physb.2005.12.078
[8] Lombardi EB, Mainwood A, Osuch K. Ab initio study of the passivation and interaction of substitutional impurities with hydrogen in diamond. Diam Relat Mater. 2003;12(3–7):490–494. doi: 10.1016/S0925-9635(02)00233-9
[9] Cheng C, Sun X, Shen W, et al. Enhancing n-type doping in diamond by strain engineering. J Phys D: Appl Phys. 2024;57(48):485103. doi: 10.1088/1361-6463/ad7270
[10] Ullah M, Ahmed E, Hussain F, et al. Electrical conductivity enhancement by boron-doping in diamond using first principle calculations. Appl Surf Sci. 2015;334:40–44. doi: 10.1016/j.apsusc.2014.07.157
[11] Ushizawa K, Watanabe K, Ando T, et al. Boron concentration dependence of Raman spectra on {100} and {111} facets of B-doped CVD diamond. Diam Relat Mater. 1998;7(11–12):1719–1722. doi: 10.1016/S0925-9635(98)00296-9
[12] Mortet V, Pernot J, Jomard F, et al. Properties of boron-doped epitaxial diamond layers grown on (110) oriented single crystal substrates. Diam Relat Mater. 2015;53:29–34. doi: 10.1016/j.diamond.2015.01.006
[13] Gabrysch M, Majdi S, Hallén A, et al. Compensation in boron-doped CVD diamond. Phys Status Solidi A. 2008;205(9):2190–2194. doi: 10.1002/pssa.200879711
[14] Zhang RJ, Lee ST, Lam YW. Characterization of heavily boron-doped diamond films. Diam Relat Mater. 1996;5(11):1288–1294. doi: 10.1016/0925-9635(96)00539-0
[15] Yap CM, Ansari K, Xiao S, et al. Properties of near-colourless lightly boron doped CVD diamond. Diam Relat Mater. 2018;88:118–122. doi: 10.1016/j.diamond.2018.07.001
[16] Volpe P-N, Pernot J, Muret P, et al. High hole mobility in boron doped diamond for power device applications. Appl Phys Lett. 2009;94(9):092102. doi: 10.1063/1.3086397
[17] Latham CD, Nieminen RM, Fall CJ, et al. Calculated properties of point defects in Be-doped GaN. Phys Rev B. 2003;67(20):205206. doi: 10.1103/PhysRevB.67.205206
[18] Zhao QX, Fimland BO, Södervall U, et al. Deactivation of Be acceptors by atomic hydrogen in AlGaAs/GaAs quantum well structures. Appl Phys Lett. 1997;71(15):2139–2141. doi: 10.1063/1.119361
[19] Van De Walle CG, Limpijumnong S, Neugebauer J. First-principles studies of beryllium doping of GaN. Phys Rev B. 2001;63(24):245205. doi: 10.1103/PhysRevB.63.245205
[20] López-Urías F, Terrones M, Terrones H. Beryllium doping graphene, graphene-nanoribbons, C60-fullerene, and carbon nanotubes. Carbon NY. 2015;84:317–326. doi: 10.1016/j.carbon.2014.11.053
[21] Ueda K, Kasu M. Beryllium-doped single-crystal diamond grown by microwave plasma CVD. Diam Relat Mater. 2009;18(2–3):121–123. doi: 10.1016/j.diamond.2008.10.009
[22] Yan CX, Dai Y, Huang BB, et al. Shallow donors in diamond: Be and Mg. Comput Mater Sci. 2009;44(4):1286–1290. doi: 10.1016/j.commatsci.2008.08.017
[23] Li C, Gao N, Li H. First-principles calculation for n-type Be P co-doping structure in diamond. Diam Relat Mater. 2025;159:112759. doi: 10.1016/j.diamond.2025.112759
[24] Zhang M, Tang K, Wu K, et al. First principles investigation on the boron-oxygen complexes in diamond. Comput Mater Sci. 2023;216:111867. doi: 10.1016/j.commatsci.2022.111867
[25] Shen S, Shen W, Liu S, et al. First-principles calculations of co-doping impurities in diamond. Mater Tod Commun. 2020;23:100847. doi: 10.1016/j.mtcomm.2019.100847
[26] Kresse G, Furthmüller J. Efficient iterative schemes for *ab initio* total-energy calculations using a plane-wave basis set. Phys Rev B. 1996;54(16):11169–11186. doi: 10.1103/PhysRevB.54.11169

[27] Blöchl PE. Projector augmented-wave method. Phys Rev B. 1994;50(24):17953–17979. doi: 10.1103/PhysRevB.50.17953
[28] Kresse G, Furthmüller J. Efficiency of ab-initio total energy calculations for metals and semiconductors using a plane-wave basis set. Comput Mater Sci. 1996;6(1):15–50. doi: 10.1016/0927-0256(96)00008-0
[29] Perdew JP, Burke K, Ernzerhof M. Generalized gradient approximation made simple. Phys Rev Lett. 1996;77(18):3865–3868. doi: 10.1103/PhysRevLett.77.3865
[30] Komsa H-P, Rantala TT, Pasquarello A. Finite-size supercell correction schemes for charged defect calculations. Phys Rev B. 2012;86(4):045112. doi: 10.1103/PhysRevB.86.045112
[31] Lany S, Zunger A. Assessment of correction methods for the band-gap problem and for finite-size effects in supercell defect calculations: case studies for ZnO and GaAs. Phys Rev B. 2008;78(23):235104. doi: 10.1103/PhysRevB.78.235104
[32] Czelej K, Śpiewak P, Kurzydłowski KJ. Electronic structure of substitutionally doped diamond: spin-polarized, hybrid density functional theory analysis. Diam Relat Mater. 2017;75:146–151. doi: 10.1016/j.diamond.2017.03.009
[33] Leslie M, Gillan NJ. The energy and elastic dipole tensor of defects in ionic crystals calculated by the supercell method. J Phys C: Solid State Phys. 1985;18(5):973–982. doi: 10.1088/0022-3719/18/5/005
[34] Feng B, Tang K, Yang K, et al. First principles investigation on the Boron-VA (VA = N, P, As, Sb) complexes in diamond for possible n-type conductivity. Mater Tod Commun. 2024;41:110266. doi: 10.1016/j.mtcomm.2024.110266
[35] Freysoldt C, Grabowski B, Hickel T, et al. First-principles calculations for point defects in solids. Rev Mod Phys. 2014;86(1):253–305. doi: 10.1103/RevModPhys.86.253
[36] Van De Walle CG, Neugebauer J. First-principles calculations for defects and impurities: applications to III-nitrides. J Appl Phys. 2004;95(8):3851–3879. doi: 10.1063/1.1682673
[37] Sun X, Shen W, Cheng C, et al. First-principles prediction of n-type diamond: novel co-doped structure using N and Be impurities. J Phys D: Appl Phys. 2024;57(21):215107. doi: 10.1088/1361-6463/ad2be1
[38] Delun Z, Tang L, Geng Y, et al. First-principles calculation to N-type Li N Co-doping and Li doping in diamond. Diam Relat Mater. 2020;110:108070. doi: 10.1016/j.diamond.2020.108070
[39] Feng B, Tang K, Yang K, et al. First principles investigation on the boron-VA (VA=N, P, as, Sb) complexes in diamond for possible n-type conductivity. Mater Today Commun. 2024; 41;110266. doi: 10.1016/j.mtcomm.2024.110266
[40] Zhang D, Sun X, Zhang Y, et al. Theoretical study on the synthetic pathway of H and N co-doped diamonds. Diam Relat Mater. 2024;149:111602. doi: 10.1016/j.diamond.2024.111602
[41] Kohn W. Nobel lecture: electronic structure of matter—wave functions and density functionals. Rev Mod Phys. 1999;71(5):1253–1266. doi: 10.1103/RevModPhys.71.1253
[42] Krukau AV, Vydrov OA, Izmaylov AF, et al. Influence of the exchange screening parameter on the performance of screened hybrid functionals. J Chem Phys. 2006;125(22):224106. doi: 10.1063/1.2404663
[43] Sun X, Zhang D, Wu G, et al. Discovery of shallow n-type scheme for boron-nitrogen co-doped diamond based on DFT calculations. Diam Relat Mater. 2025;153:112041. doi: 10.1016/j.diamond.2025.112041